MethodsX 13 (2024) 102919

Contents lists available at ScienceDirect

MethodsX

journal homepage: www.elsevier.com/locate/methodsx

Utilizing decellularized bio-membranes to optimize histopathological embedding of small tissues

Jinyang Li [a,b,†], Yanyan Zhou [c,†], Tianyou Luo [d], Hongzhen Mao [a], Lijuan Yin [d], Yuanfa Zhang [c], Tianyi He [c], Yang Deng [c], Fei Chen [c], Zuoyu Liang [c], Li Li [c], Lili Jiang [d], Ji Bao [a,*]

[a] *Department of Pathology, Institute of Clinical Pathology, Key Laboratory of Transplant Engineering and Immunology, NHC, West China Hospital, Sichuan University, Chengdu 610041, China*
[b] *Department of Pathology, Regeneration Medicine Research Center, West China Hospital, Sichuan University, Chengdu 610041, China*
[c] *Institute of Clinical Pathology, West China Hospital, Sichuan University.*
[d] *Department of Pathology, West China Hospital, Sichuan University, Chengdu, 610041, China*

A R T I C L E I N F O

Method name:
Method for direct paraffin embedding of small tissues with decellularized biomembrane materials.

Keywords:
Decellularization
Microtissues
Organoids
Paraffin embedding
Pathology preparation

A B S T R A C T

In recent years, minimally invasive biopsy techniques have been widely used to generate small tissue samples that require processing in clinical pathology. However, small paraffin-embedded tissues are prone to loss due to their small size. To prevent the loss of small tissues, researchers have employed nonbiological embedding materials for preembedding, but this approach can lead to cumbersome experimental procedures and increase the chances of tissue loss. This study aimed to develop a convenient decellularized embedding material derived from biological membrane tissues to effectively protect small tissues from loss during paraffin embedding. This study decellularized three types of fresh animal-derived membrane tissues and selected the small intestine as the most suitable decellularized raw material through attempts at softening, comparing physical properties, and using tissue as the starting material. Subsequently, small tissues from various tissue sources were embedded, followed by H&E staining, Masson staining, immunofluorescence staining, and immunohistochemical staining. The decellularized material derived from biomembrane tissues (DMBT) developed in this study can reduce the loss of small tissues without the need for preembedding, thereby shortening the embedding process. This provides a new pathological embedding tool for future laboratory and clinical research and work.

- The fat layer of the pig's small intestine is scraped off, and chemical reagents are used to defat and decellularize it.
- Chemical reagents are used to soften and make the pig's small intestine transparent, and the decellularized pig's small intestine is dried.
- DMBT is used for embedding and staining the biological tissue.

* Corresponding author. Ji Bao, Department of Pathology, Institute of Clinical Pathology, Key Laboratory of Transplant Engineering and Immunology, NHC, West China Hospital, Sichuan University, No. 37, Guoxue Alley, Wuhou District, Chengdu 610041, Sichuan Province, China
E-mail address: baoji@scu.edu.cn (J. Bao).
† These authors contributed equally.

https://doi.org/10.1016/j.mex.2024.102919
Received 7 July 2024; Accepted 15 August 2024
Available online 20 August 2024

Specifications table

Subject area:	Materials Science
More specific subject area:	*Decellularization of biological tissues*
Name of your method:	*Decellularization of biological tissues, pathological embedding*
Name and reference of original method:	*Casarin, M.; Fortunato, T. M.; Imran, S.; Todesco, M.; Sandrin, D.; Borile, G.; Toniolo, I.; Marchesan, M.; Gerosa, G.; Bagno, A.; Romanato, F.; Carniel, E. L.; Morlacco, A.; Dal Moro, F., Porcine Small Intestinal Submucosa (SIS) as a Suitable Scaffold for the Creation of a Tissue-Engineered Urinary Conduit: Decellularization, Biomechanical and Biocompatibility Characterization Using New Approaches. 2022, 23 (5), 2826.* *Kao, C. Y.; Nguyen, H. Q.; Weng, Y. C., Characterization of Porcine Urinary Bladder Matrix Hydrogels from Sodium Dodecyl Sulfate Decellularization Method. Polymers (Basel) 2020, 12 (12).* *14. Bai, H.; Sun, P.; Wu, H.; Wei, S.; Xie, B.; Wang, W.; Hou, Y.; Li, J.; Dardik, A.; Li, Z., The application of tissue-engineered fish swim bladder vascular graft. Commun Biol 2021, 4 (1), 1153.*
Resource availability:	*Not applicable*

Background

In recent years, ultrasound-guided fine needle aspiration biopsy has been widely used for minimally invasive examination, offering advantages such as high safety, accuracy, minimal invasiveness, and few complications [1,2]. This biopsy technique is extensively applied in clinical pathology, generating numerous small tissue biopsy samples from various locations, including the thyroid, prostate, breast, lymph nodes, pancreas, and hepatobiliary system [3-5]. These small specimens provide valuable pathological information for clinicians and play a crucial role in the accurate diagnosis and treatment of diseases. For the clinical pathological examination of these small tissues, paraffin embedding is an important technique.

Although significant progress has been made by researchers in handling conventional and large tissue samples, challenges persist when dealing with small tissue samples [6]. Tissues obtained through biopsies typically have characteristics such as a small sample size, irregular shape, fragile texture, and tendency to float in liquids[7]. In order to enable the embedding of tiny biopsy tissues, researchers have developed a variety of materials for the encapsulation of tiny tissues, thereby preventing the loss of tiny tissues during paraffin embedding. Existing conventional paraffin embedding materials for small tissues include gauze, lens paper, and filter paper, which are primarily used to wrap small tissues in advance in embedding boxes to protect them during sectioning [8-10]. However, these materials are cumbersome to handle and often lead to sample loss, missed sections, and difficulties in placing multiple small tissues on the same plane for observation. These challenges make the advancement of related research more challenging. Therefore, further optimization and innovation of techniques for handling small tissues are urgently needed to meet the growing demands of both research and clinical practice.

Therefore, there is a need to develop a novel embedding material specifically for small and fragile tissues, such as small rodent organs and human tissue biopsies. This new material should be ready-to-use and should not produce nonspecific background staining during histopathological sectioning. Additionally, it should possess good biocompatibility and stable physical properties to ensure that tissue samples are not damaged during sectioning. Therefore, we are considering the use of decellularized materials derived from biological sources. Compared to non-biological sources such as filter paper or silk cloth, decellularized materials can bypass the pre-embedding step. This eliminates the need to remove wrapping materials, such as filter paper or silk cloth, allowing for direct embedding, followed by subsequent sectioning and staining, thereby accelerating the experimental process.

In this study, we achieved efficient decellularization of three widely accessible fresh tissues (pig bladder, pig small intestine, and fish swim bladder). Through comprehensive evaluation of parameters such as DNA content, material thickness, and tensile strength, we selected decellularized biological membrane material derived from the pig small intestine as the embedding material for small tissues. This material effectively replaces existing embedding materials and circumvents the main drawbacks associated with them. In practical applications, this material has been successfully used to embed various types of small tissues without causing tissue loss. The histopathological sections produced using this material demonstrated high tissue integrity. Furthermore, this material is compatible not only with H&E and special stains but also with immunohistochemical staining and immunofluorescence staining, with no adverse effects on the staining results. This method significantly improves the quality of histopathological sections of small tissue biopsies and effectively prevents sample loss during sectioning. Its simplicity of operation and suitability for routine pathology laboratories, without the need for specialized equipment and reagents, make this novel decellularized biological membrane tissue material (DBMT) a convenient and efficient embedding tool for researchers.

Methods in detail

Decellularization of fresh membrane tissues

Decellularization of fresh pig small intestines.

1) Fresh pig small intestines were purchased from the market, and the fat was removed. The intestines were then cut along the midline into rectangular pieces approximately 15 cm in length. The other layers of the small intestine were scraped off, leaving only the submucosal layer. The tissue was washed repeatedly with phosphate-buffered saline (PBS) (HyClone, USA).
2) A defatting solution was prepared by mixing methanol (Kelong Chemical, China) and chloroform (Kelong Chemical, China) in equal volumes. The small intestine was transferred to the defatting solution and defatted at room temperature for 12 h.

3) The tissue was washed three times with PBS (Gibco, USA) and then five times with double-distilled water. The defatted small intestine was subjected to decellularization using 0.25 % trypsin (Gibco, USA) at 4 ˚C for 12 h, followed by five washes with double-distilled water.
4) Subsequently, the tissue was treated with 0.5 % SDS (Promega, USA) solution for additional decellularization, shaken on a shaker (80 PRM) at room temperature for 4 h, and then washed five times with double-distilled water to remove residual reagents thoroughly [11].

Decellularization of fresh pig bladders.

1) Fresh pig bladders were purchased from the market, and the outer fat tissue and fibrous connective tissue were removed. The bladder was washed with physiological saline to remove epithelial cells. Subsequently, the bladder was cut into rectangular pieces approximately 15 cm in length.
2) The bladder pieces were immersed in a decellularization solution containing 0.025 % trypsin and 0.05 % EDTA and then placed on a shaker at a constant temperature of 37 ˚C. To ensure thorough mixing and reaction between the samples and the solution, the shaker was set to oscillate at 200 rpm for 1 hour. The bladder pieces were then washed five times with double-distilled water, with each wash lasting 30 min.
3) Next, the bladder pieces were transferred to a 3 % Triton X-100 (Amresco, USA) solution and shaken on a shaker at 200 rpm for 1 hour. Afterward, the bladder pieces were washed five times with double-distilled water, with each wash lasting 30 min.
4) Finally, the bladder pieces were transferred to a 4 % deoxycholic acid (Biosharp, China) solution and shaken on a shaker (80 PRM) for 1 hour. The bladder pieces were washed five times with double-distilled water for 30 min each time to remove residual reagents completely [12,13].

Decellularization of fresh fish swim bladders.

1) Fresh fish swim bladders were purchased from the market, and the surrounding fat was removed. The swim bladder is cut along the median line, dividing it into two hemispherical membranes of equal size.
2) The swim bladders were placed in 500 mL of CHAPS buffer solution (containing 8 mM CHAPS (Macklin, China), 1 M NaCl (Kelong Chemical, China), and 25 mM EDTA (Biofroxx, Germany)) and incubated for 12 h. The swim bladders were washed three times in PBS for 60 min each.
3) Subsequently, the swim bladders were placed in 500 mL of SDS solution (containing 1.8 mM SDS, 1 M NaCl, and 25 mM EDTA in PBS) and incubated for 24 h. Then, the swim bladders were washed five times with PBS to completely remove residual reagents [14,15] (Fig. 1).

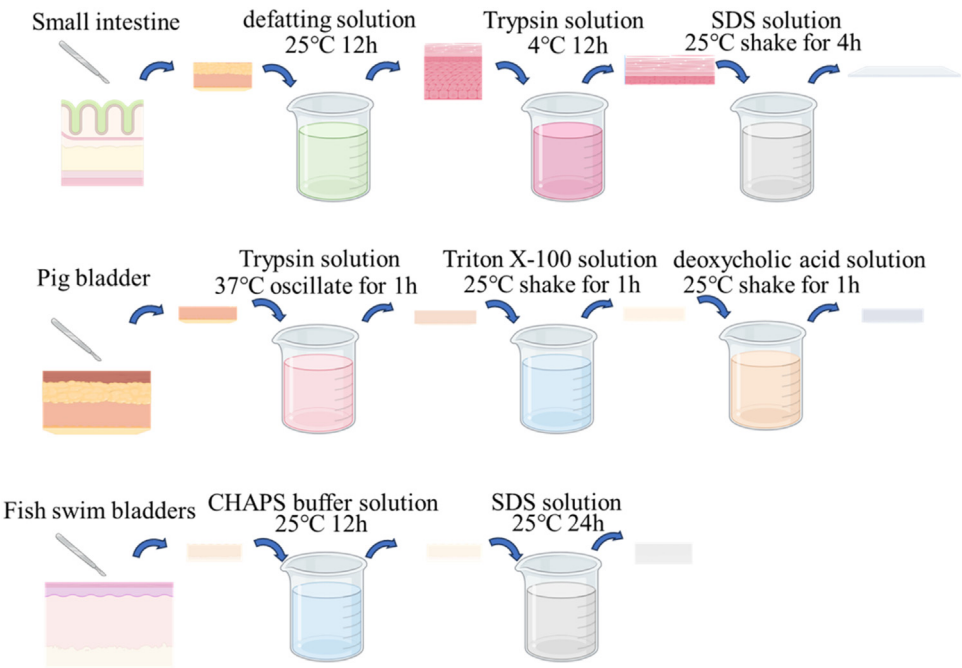

Fig. 1. Decellularization of fresh membrane tissues.

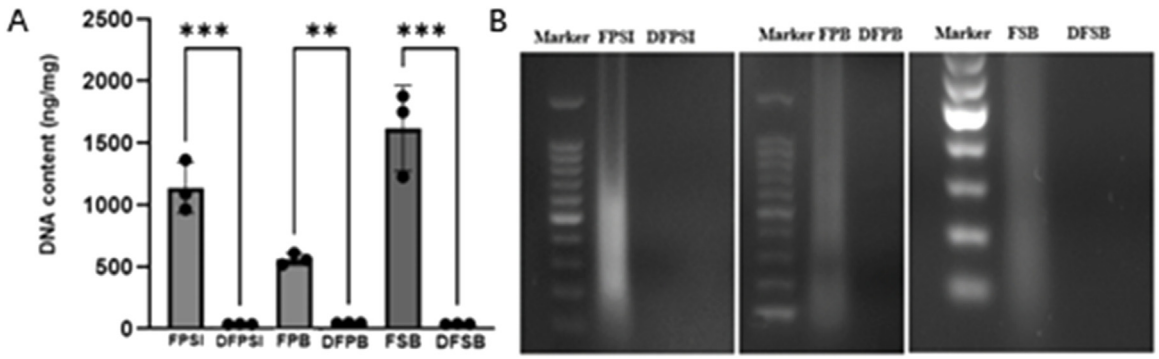

Fig. 2. Evaluation the DNA content of the decellularized tissue (A) DNA content of fresh tissues and decellularized fresh tissues; (B) Agarose gel electrophoresis of fresh tissues and decellularized fresh tissues. FPSI: fresh pig small intestine, DFPSI: decellularized fresh pig small intestine, FPB: fresh bladder, DFPB: decellularized fresh bladder, FSB: fresh swim bladder, DFSB: decellularized fresh swim bladder.

Molecular biology of decellularized fresh biological membrane materials

The fresh tissues and decellularized tissues were dried in a 37 ˚C oven for 2 h and ground into powder with liquid nitrogen, and 10 mg of dried fresh tissues, dried tissues, and decellularized tissues were weighed on an electronic balance and transferred to centrifuge tubes. DNA extraction was performed using a DNA extraction kit (Tiangen, China). A 1 μL DNA sample was taken for concentration determination using a NanoDrop 2000 (Thermo, USA), and its DNA content was measured. A 1.5 % agarose gel solution (Tsingke, China) was prepared, and Gel Red nucleic acid dye (Tsingke, China) was added to a volume of 0.01 % agarose solution. After the agarose gel solidified, 5 μL of DNA was mixed with 1 μL of loading buffer (Tsingke, China) and then loaded into one lane along with a DL2000 Maker (Tsingke, China) for agarose gel electrophoresis.

In decellularization-based studies, the success of removing genomic components is typically evaluated using the following criteria: <50 ng of double-stranded DNA (dsDNA) per mg dry weight of extracellular matrix (ECM), DNA fragment lengths <200 bp, and the absence of visible nuclear material upon DAPI staining [16].

The DNA content of fresh small intestine tissue was found to be 1139±204.16 ng/mg, while that of decellularized fresh small intestine tissue was 35.33±1.53 ng/mg, which was significantly lower than 50 ng. Decellularization led to a significant reduction in the DNA content of fresh small intestine tissues ($P < 0.001$). Similarly, the DNA content of fresh bladder tissue was 560.3 ± 46.2 ng/mg, while that of decellularized fresh bladder tissue was 44.67±2.5 ng/mg, indicating a significant decrease in DNA content ($P < 0.01$) following decellularization. The DNA content of fresh fish swim bladder tissue was 1618±344.5 ng/mg, whereas that of decellularized fish swim bladder tissue was 37.1 ± 2.1 ng/mg, demonstrating a significant reduction in DNA content ($P < 0.001$) after decellularization. The DNA content of decellularized tissues complied with the criteria for decellularization, ensuring <50 ng of dsDNA per mg dry weight of ECM (Fig. 2A).

Agarose gel electrophoresis analysis of DNA extracted from fresh tissues and decellularized tissues derived from fresh tissues revealed distinct DNA bands in fresh small intestine, bladder, and fish swim bladder tissues, while no bands were observed in decellularized tissues (Fig. 2B).

Processing of DMBTs suitable for pathological embedding and sectioning

1) A transparent solution containing 10% N,N-diethyl ethanolamine (Macklin, China), 10 % Triton X-100, and 80 % double-distilled water was prepared. The decellularized tissues were placed in 100 mL of the transparent solution and shaken on a shaker for 12 h. The tissues were washed three times with PBS.
2) A digestion solution containing 1 mg/mL pepsin (Sigma, USA) in double-distilled water was prepared, and the decellularized, softened tissues were immersed in the digestion solution. The mixture was shaken for 2 h or acidified overnight with 2 equivalents of hydrochloric acid (Kelong Chemical, China). The cells were washed three times with PBS [17].
3) The tissue surface was blotted dry with absorbent paper, the decellularized small intestines and bladders were laid flat in smooth plastic containers, and the decellularized swim bladders were wrapped in approximately 15 mL centrifuge tubes.
4) The tissues were placed in a 37 ˚C oven and allowed to dry for 45–60 min until completely dry. The resulting DMBT is suitable for long-term storage and pathological embedding.

Histological examination of decellularized fresh biological membrane materials

The tissues were fixed in 10 % neutral formalin solution (Kelong Chemical, China) for 48 h. The tissues were then dehydrated, clarified, embedded in paraffin, sectioned(the thickness of the tissue slices is 3–5μm), and deparaffinized using an automatic dehydration machine (Thermo, USA).

HE staining

1) The sections were stained with hematoxylin-eosin dye (Baso Biological, China) by immersing them in hematoxylin dye solution for 5 min, followed by a 5-minute wash in double-distilled water.
2) Subsequently, the sections were dipped in hydrochloric acid alcohol solution for 1 min, washed for 1 min in double-distilled water, and then stained with eosin dye solution for 1 min.
3) The sections were dehydrated in a gradient of alcohol, clarified with xylene (Kelong Chemical, China), mounted, and observed under an optical microscope.

For Masson staining, tissue staining was performed using a modified Masson's trichrome staining kit (Solarbio, China), and staining was carried out according to the manufacturer's instructions. Finally, dehydration was carried out using 95 % and absolute ethanol, followed by clearing with xylene, mounting, and observation under an optical microscope.

For DAPI staining, the tissue was covered with 50 μL of DAPI staining solution (Sigma, USA) and incubated at room temperature in the dark for 5 min. The excess DAPI staining solution was removed by washing with double-distilled water, the slides were mounted with glycerol, and the slides were observed under a fluorescence microscope.

Immunofluorescence Staining

1) Citrate antigen retrieval solution (MXB Biotechnologies, China) was prepared at a ratio of 1:100 in water, and the solution was added to the retrieval tank.
2) The slides were placed in a tank and heated in a 67 ˚C water bath for 2 h.
3) The slides were washed with wash buffer, placed in a humid box, mixed with a drop of animal nonimmune serum (MXB Biotechnologies, China), and incubated at room temperature for 10 min.
4) The serum was discarded, the primary antibodies (Dako, Denmark) were diluted in antibody dilution buffer, and specific primary antibodies, including a laminin antibody (ab11575, Abcam, UK), were added to the paraffin sections according to the manufacturer's instructions.
5) The mixture was incubated overnight at 4 ˚C.
6) The slides were washed with wash buffer (Dako, Denmark), and the paraffin sections were incubated with biotinylated goat anti-mouse/rabbit IgG secondary antibodies (Invitrogen, USA) at 37 ˚C for 1 hour.
7) Then, 60 μL of DAPI was added, the cells were stained for 5 min, washed, mounted with glycerol, and observed under a fluorescence microscope.

Immunohistochemical Staining

1) EDTA antigen retrieval solution was added to the retrieval tank, the slides were placed in the tank, and high-temperature retrieval was performed in a 67 ˚C water bath for 2 h.
2) After washing, a drop of animal nonimmune serum was added to the paraffin sections, and nonspecific antigens were blocked for 10 min.
3) The primary antibodies (Dako, Denmark) were diluted in antibody dilution buffer, and specific primary antibodies, such as Ki-67 (ab16667, Abcam, UK), were added to the paraffin sections. The slides were placed in a humid box and incubated overnight at 4 ˚C, followed by washing.
4) The secondary antibody working solution was added and incubated at 37 ˚C for 1 hour.
5) After washing, DAB chromogenic solution was added to the slides, and the staining time was controlled under a microscope.
6) After washing, the sections were stained with hematoxylin dye solution for 5 min, differentiated with hydrochloric acid alcohol for 10 s, dehydrated with an alcohol gradient, air-dried, and covered with a glass coverslip.

Scanning electron microscopy (SEM)

1) Fresh tissues were immersed in 2.5 % glutaraldehyde (Kelong Chemical, China) and fixed at 4 ˚C for 12 h, followed by washing with PBS and dehydration with an alcohol gradient.
2) Subsequently, the tissues were dried using a critical point dryer (Leica, Germany) for 52 min.
3) The samples were fixed onto metal stubs with conductive carbon tape and sputter-coated with gold for 90 s using an ion sputter coater.
4) The material surfaces were observed using a scanning electron microscope (Zeiss, Germany).

The decellularization method we used is shown in the Fig. 3. Fresh porcine small intestines exhibit a pale brown color, are curved, and possess elasticity; after decellularization, they appear milky white with an intact structure. Fresh bladder tissue is light yellow with abundant muscular tissue; postdecellularization, it becomes semitransparent and retains good elasticity. The swim bladder is white when fresh, with a dense structure; after decellularization, the fiber content is reduced, and the extracellular matrix (ECM) remains intact. H&E staining revealed that decellularization removed the cell nuclei, leaving only the extracellular matrix (ECM). Masson's staining highlights the abundance of collagen fibers and muscle fibers, while DAPI staining and SEM analysis confirm the effectiveness of decellularization.

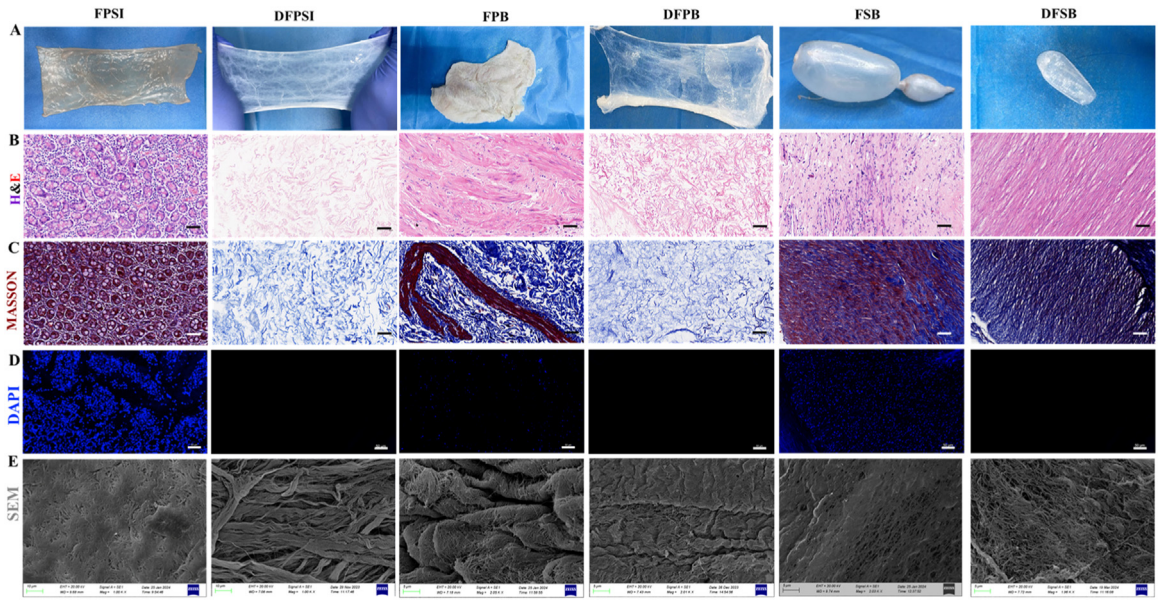

Fig. 3. Histological and SEM examination of decellularized tissues (A) Morphological images of fresh and decellularized tissues; (B) H&E staining of fresh and decellularized tissues; scale bar: 50 μm. (C) Masson staining of fresh and decellularized tissues, where collagen is blue–purple, the cytoplasm is pink, and the nucleus is dark blue or black; scale bar: 50 μm. (D) DAPI staining of fresh and decellularized tissues; scale bar: 50 μm. (E) SEM images of fresh and decellularized tissues, with scale bars of 10 μm for FPSI/DFPSI and 5 μm for FPB/DFPB/FSB/DFSB. FPSI: fresh pig small intestine, DFPSI: decellularized fresh pig small intestine, FPB: fresh bladder, DFPB: decellularized fresh bladder, FSB: fresh swim bladder, DFSB: decellularized fresh swim bladder.

Physical and mechanical properties of the DMBT

Measurement of Thickness: The thickness of the samples was determined using a rotary screw micrometer (Delixi, China). The probe was gradually brought close to the surface of the sample until contact was made, and measurements were recorded. Three different locations were selected from each sample, and the average of these measurements was calculated.

Tensile Strength Measurement: Rectangular specimens approximately 35 mm in length and 25 mm in width were cut from the material. The specimens were mounted onto a tensile testing machine (Shanghai Rixi Electronic Technology Co., Ltd., China), and the gauge length was measured. The tensile testing machine was set to start moving at a loading speed of 5 mm/min. Measurements were stopped upon reaching the breaking point, and based on the obtained stress–strain data, the tensile properties of the samples were calculated. Three samples were measured for each group, and the average value was taken.

To investigate which type of decellularized material and which softening method (pepsin or hydrochloric acid) is most suitable for subsequent embedding, we softened these three tissues using two different softening methods. The results showed that the material softened with pepsin for the small intestine had a lower thickness and tensile strength, making it most suitable for subsequent embedding (Fig. 4).

Preparation of microtissues

All animal procedures were conducted in compliance with the Laboratory Animal Welfare Act guidelines and standard operating procedures at the Sichuan University Research Center, with approval from the Animal Experiment Center of Sichuan University.

After the rats were weighed, an overdose of sodium pentobarbital (50 mg kg^{-1}) was intramuscularly injected. The abdominal skin was disinfected with iodine, and a large area was shaved. Following the placement of sterile surgical drapes over the abdominal area, a midline incision was made, and various shapes of microtissues, including the heart, spleen, and kidney, were dissected into pieces smaller than 2 mm in length and soaked in a large volume of 4 % paraformaldehyde solution (Biosharp, China) for >24 h for fixation. Breast cancer tumor tissues were donated by Xinyi Long, and the preparation method involved subcutaneous implantation of 1 × 10 [7] MDA-MB-231 cells into female BALB/c mice. When the tumor volume reached 1000 mm [3], the mice were euthanized, and the tumors were collected. Mouse liver tissues were donated by Gang Liu from Inner Mongolia Medical University.

Embedding of microtissues in the DMBT

Embedding of Microtissues: Microtissues were placed in wetted DMBTs, and the folding method was employed to prevent leakage of microtissues during transfer into embedding cassettes (Fig. 5).

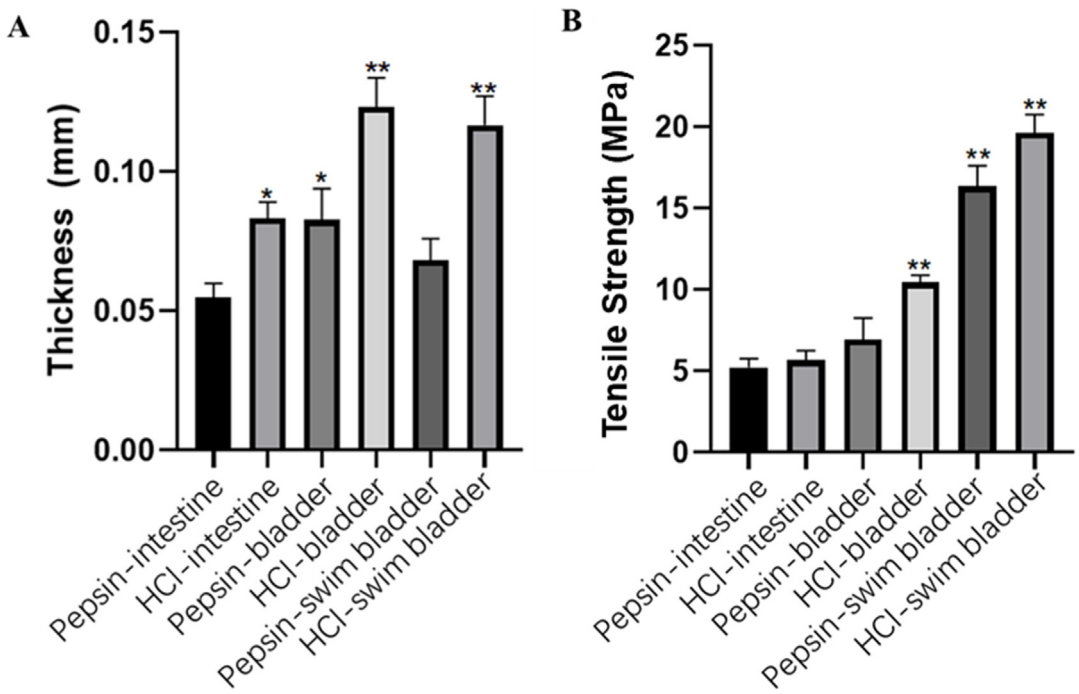

Fig. 4. Thickness and tensile strength of the DMBT. (A) Thickness of decellularized tissues softened by pepsin or hydrochloric acid. (B) Tensile strength of decellularized tissues softened by pepsin or hydrochloric acid after drying. * indicates $P < 0.05$ compared to the pepsin-intestine group, ** indicates $P < 0.01$ compared to the pepsin-intestine group.

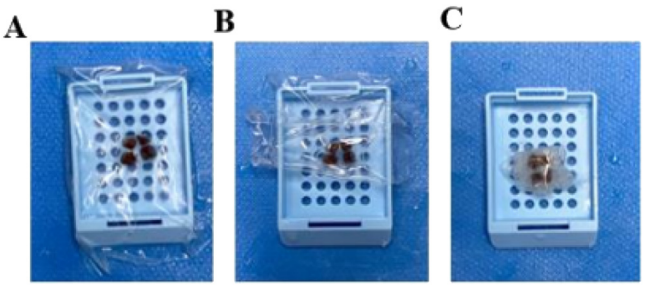

Fig. 5. Diagram of decellularized small intestinal embedded microtissues. (A) Microtissues are placed in the center of a decellularized biofilm material moistened with formalin; (B) DMBT folds from the periphery to the middle; (C) The decellularized biofilm material completely encapsulates the tiny tissues and fastens the lid.

Using the method described in section 2.3, the embedded tissues were sliced and stained with HE, Masson's trichrome, immunohistochemistry, and immunofluorescence.

The experimental results, in the Fig. 6, indicate that tissue sections embedded with DMBT did not exhibit cutting marks, demonstrating that DMBT does not affect the sectioning process. Following H&E staining and Masson staining, the tissue structure on the pathological sections remained well preserved, indicating that embedding decellularized tissue did not alter the intrinsic structure of the tissue. The staining effects were clear and vivid, with a uniform distribution of cardiomyocytes, hepatocytes, renal cells, and splenic cells, without any noticeable loss or abnormalities in cell distribution. Furthermore, the results from immunofluorescent and immunohistochemical staining further confirmed that DMBT embedding in small tissues does not affect the intrinsic spatial specificity of protein expression in the tissue.

Statistical analysis

Statistical analysis was performed using GraphPad Prism v8.0 (t-test). All the data are presented as the mean ± SEM. Values were considered statistically significant at $p < 0.05$. The results represent three or more independent experiments.

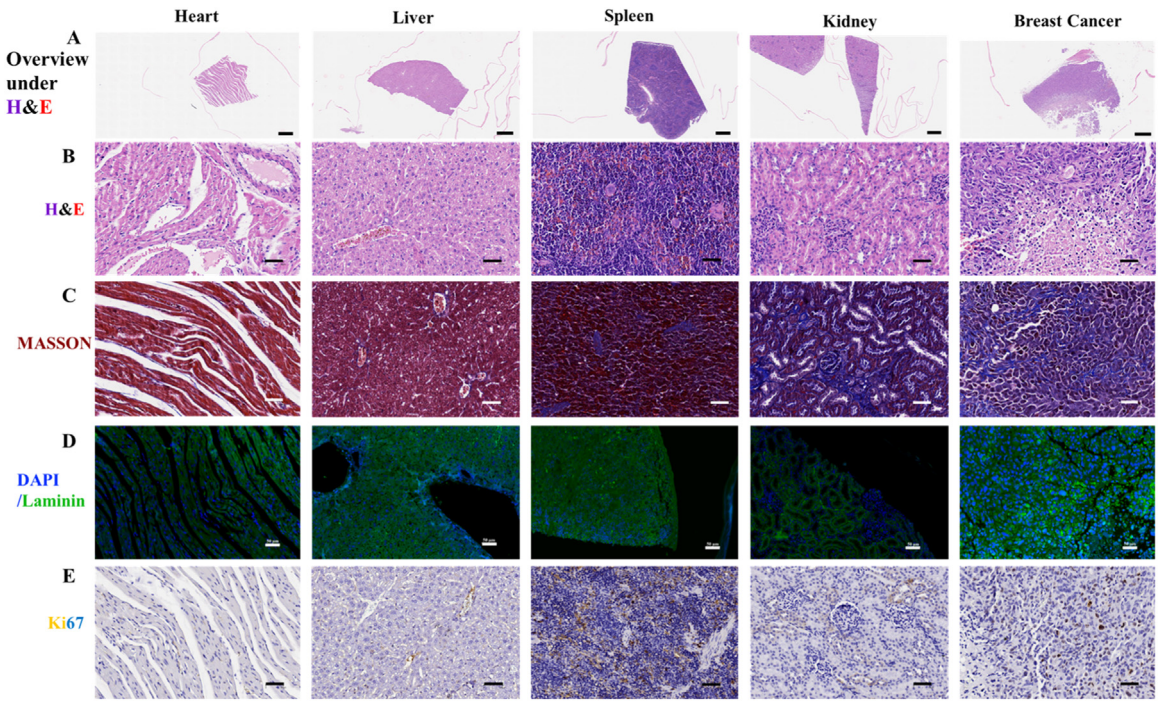

Fig. 6. DMBT used for embedding microscopic tissues. From left to right, microscopy images of tissues from mouse heart, liver, spleen, kidney, and mouse mammary tumors are shown. (A) The tissue and decellularized embedding material were observed under low magnification after H&E staining; scale bar: 500 μm. (B) H&E staining of microscopic tissues embedded in decellularized dehydrated intestinal tissue; scale bar: 50 μm. (C) Masson staining of microscopic tissues embedded in decellularized dehydrated intestinal tissue, where collagen is blue–purple, the cytoplasm is pink, and the nucleus is dark blue or black; scale bar: 50 μm. (D) DAPI/Laminin staining of microscopic tissues embedded in decellularized dehydrated intestinal tissue (blue: DAPI, green: laminin); scale bar: 50 μm. (E) Immunohistochemical staining of Ki-67 in microscopic tissues embedded in decellularized dehydrated intestinal tissue, where the Ki-67 protein is shown in brown; scale bar: 50 μm.

Conclusion

This study investigated partially decellularized biological membrane tissues and optimized methods for tissue softening. We compared the physicochemical properties of biological membrane tissues after decellularization and ultimately selected and developed decellularized intestinal membranes as embedding materials for small tissues. This shortened the traditional embedding process. We embedded various tissues from multiple sources and subjected them to H&E, Masson's trichrome, immunofluorescence, and immunohistochemical staining.

Declaration of competing interest

The authors declare no conflicts of interest.

CRediT authorship contribution statement

Jinyang Li: Validation, Data curation. **Yanyan Zhou:** Conceptualization. **Tianyou Luo:** Methodology. **Hongzhen Mao:** Validation, Writing – original draft, Writing – review & editing. **Lijuan Yin:** Funding acquisition. **Yuanfa Zhang:** Formal analysis. **Tianyi He:** Writing – original draft. **Yang Deng:** Resources. **Fei Chen:** Visualization. **Zuoyu Liang:** Conceptualization. **Li Li:** Supervision. **Lili Jiang:** Software. **Ji Bao:** Investigation, Project administration, Funding acquisition.

Data availability

Data will be made available on request.

Funding

This research was funded by the National Natural Science Foundation of China (82270662, 82070640), the Technology Innovation Project of Chengdu New Industrial Technology Research Institute (2018-CY02–00046-GX), the 1.3.5 Project for Disciplines

of Excellence, West China Hospital, Sichuan University (No. ZYIC21014), and the Sichuan Provincial Natural Science Foundation Project (2022NSFSC1390).

Acknowledgments

This study would like to express gratitude to Li, Fei Chen, Yuanfa Zhang, and Chuanjuan Bao for their support and guidance throughout this research.

References

[1] P. Kandel, M.B. Wallace, Optimizing endoscopic ultrasound guided tissue sampling of the pancreas, JOP J. Pancreas 17 (2016) 160–165.
[2] P. Kandel, M.B. Wallace, Recent advancement in EUS-guided fine needle sampling, J. Gastroenterol. 54 (5) (2019) 377–387.
[3] C. Tourasse, E. Khasanova, P. Sebag, J.P. Beregi, Ultrasound-guided vacuum-assisted breast biopsy with a small-caliber device: a multicenter consecutive study of 162 biopsied lesions, Tumori. 105 (4) (2019) 312–318.
[4] T. Sakaguchi, Y. Nishii, A. Iketani, S. Esumi, M. Esumi, K. Furuhashi, Y. Nakamura, Y. Suzuki, K. Ito, K. Fujiwara, K. Katsuta, O. Taguchi, O. Hataji, Comparison of the analytical performance of the Oncomine dx target test focusing on bronchoscopic biopsy forceps size in non-small cell lung cancer, Thorac. Cancer 13 (10) (2022) 1449–1456.
[5] L. Yarmus, J. Akulian, C. Gilbert, D. Feller-Kopman, H.J. Lee, P. Zarogoulidis, N. Lechtzin, S.Z. Ali, V. Sathiyamoorthy, Optimizing endobronchial ultrasound for molecular analysis. How many passes are needed?, in: Ann. Am. Thorac. Soc., 10, 2013, pp. 636–643.
[6] O. Zhanmu, X. Yang, H. Gong, X. Li, Paraffin-embedding for large volume bio-tissue, Sci. Rep. 10 (1) (2020) 12639.
[7] P.A. VanderLaan, H.H. Wang, A. Majid, E. Folch, Endobronchial ultrasound-guided transbronchial needle aspiration (EBUS-TBNA): an overview and update for the cytopathologist, Cancer Cytopathol. 122 (8) (2014) 561–576.
[8] D. Cao, X. Ma, W.J. Zhang, Z. Xie, Dissection and coronal slice preparation of developing mouse pituitary gland, J. Vis. Exp. (129) (2017).
[9] H.L. Dai, M.Y. Tan, L.M. Guo, Study on absorbency and strength of the carboxymethyl medical cotton gauze, Adv. Mat. Res. 821 (2013) 502–510.
[10] S. Golan, G. Gerber, D. Margel, L. Rath-Wolfson, Y. Ehrlich, R. Koren, D. Lifshitz, A novel technique to improve the processing of minute ureteroscopic biopsies, Pathol. Oncol. Res. 24 (1) (2018) 89–94.
[11] Casarin, M., Fortunato, T.M., Imran, S., Todesco, M., Sandrin, D., Borile, G., Toniolo, I., Marchesan, M., Gerosa, G., Bagno, A., Romanato, F., Carniel, E.L., Morlacco, A.; Dal Moro, F., Porcine small intestinal submucosa (SIS) as a suitable scaffold for the creation of a tissue-engineered urinary conduit: decellularization, biomechanical and biocompatibility characterization using new approaches. 2022, 23 (5), 2826.
[12] C.Y. Kao, H.Q. Nguyen, Y.C. Weng, Characterization of porcine urinary bladder matrix hydrogels from sodium dodecyl sulfate decellularization method, Polymers. (Basel) (12) (2020) 12.
[13] J. Liao, Q. Guo, B. Xu, X. Li, Overview of decellularized materials for tissue repair and organ replacement, in: X. Li, H. Xie (Eds.), Decellularized materials, Springer Singapore, Singapore, 2021, pp. 1–67.
[14] H. Bai, P. Sun, H. Wu, S. Wei, B. Xie, W. Wang, Y. Hou, J. Li, A. Dardik, Z. Li, The application of tissue-engineered fish swim bladder vascular graft, Commun. Biol. 4 (1) (2021) 1153.
[15] A. Neishabouri, A. Soltani Khaboushan, F. Daghigh, A.M. Kajbafzadeh, M. Majidi Zolbin, Decellularization in tissue engineering and regenerative medicine: evaluation, modification, and application methods, Front. Bioeng. Biotechnol. 10 (2022) 805299.
[16] P.M. Crapo, T.W. Gilbert, S.F. Badylak, An overview of tissue and whole organ decellularization processes, Mater. Sci., Biomater. - SCIE(Q1); Eng., Biomed. - SCIE(Q1) 32 (12) (2011) 3233–3243.
[17] G. Cao, X. Li, The decellularization of tissues, in: X. Li, H. Xie (Eds.), Decellularized materials, Springer Singapore, Singapore, 2021, pp. 69–114.